Available online at www.sciencedirect.com
SCIENCE DIRECT®
Biochemical Pharmacology 65 (2003) 1435–1439
Biochemical Pharmacology
www.elsevier.com/locate/biochempharm

Molecular mechanisms for the activation of Ca^{2+}-permeable nonselective cation channels by endothelin-1 in C6 glioma cells

Yoshifumi Kawanabe[a,b,*], Nobuo Hashimoto[a], Tomoh Masaki[b]

[a]*Department of Neurosurgery, Kyoto University Graduate School of Medicine, Kyoto 606-8507, Japan*
[b]*Department of Pharmacology, Kyoto University Graduate School of Medicine, Kyoto 606-8507, Japan*

Received 3 May 2002; accepted 18 October 2002

Abstract

We recently demonstrated that endothelin-1 (ET-1) activates two types of Ca^{2+}-permeable nonselective cation channels (NSCC-1 and NSCC-2) in C6 glioma cells. It is possible to discriminate between these channels by using the Ca^{2+} channel blockers SK&F 96365 (1-[β-(3-[4-methoxyphenyl]propoxy)-4-methoxyphenethyl]-1*H*-imidazole hydrochloride) and LOE 908 [(*R*,*S*)-(3,4-dihydro-6,7-dimethoxy-isoquinoline-1-yl)-2-phenyl-*N*,*N*-di-[2-(2,3,4-trimethoxyphenyl)ethyl]-acetamide]. LOE 908 is a blocker for NSCC-1 and NSCC-2, whereas SK&F 96365 is an inhibitor for NSCC-2. The purpose of the present study was to identify the G-proteins that are involved in ET-1-activated Ca^{2+} channels in C6 glioma cells. ET-1 activated only NSCC-1 in C6 glioma cells preincubated with U73122 (1-[6-[((17β)-3-methoxyestra-1,3,5[10]-trien-17-yl)amino]hexyl]-1*H*-pyrrole-2,5-dione), a phospholipase C (PLC) inhibitor. Microinjection of the dominant negative mutant of G_{12}/G_{13} (G_{12}G228A/G_{13}G225A) abolished activation of NSCC-1 and NSCC-2. In contrast, pertussis toxin did not affect any of the Ca^{2+} channels in the ET-1-stimulated C6 glioma cells. These results indicate that G_{12}/G_{13} may couple with endothelin receptors and play an important role in the activation of NSCCs in C6 glioma cells. Moreover, the activation mechanisms of NSCC-1 and NSCC-2 by ET-1 were different. NSCC-1 activation depended upon a G_{12}/G_{13}-dependent cascade, whereas NSCC-2 activation depended upon both G_q/PLC- and G_{12}/G_{13}-dependent cascades.

Keywords: Endothelin; Nonselective cation channel; G-protein; C6 glioma

1. Introduction

ET-1 acts as a neurotransmittor [1] and induces cell proliferation [2]. We have shown recently that the ET-1-induced sustained increase in $[Ca^{2+}]_i$ results in Ca^{2+} entry through two types of Ca^{2+}-permeable NSCCs (designated NSCC-1 and NSCC-2) in C6 glioma cells [2]. These channels can be distinguished by using the Ca^{2+} channel blockers SK&F 96365 (1-[β-(3-[4-methoxyphenyl]propoxy)-4-methoxyphenethyl]-1*H*-imidazole hydrochloride) and LOE 908 [(*R*,*S*)-(3,4-dihydro-6,7-dimethoxy-isoquinoline-1-yl)-2-phenyl-*N*,*N*-di-[2-(2,3,4-trimethoxyphenyl)-ethyl]-acetamide]. NSCC-1 is sensitive to LOE 908 and resistant to SK&F 96365. NSCC-2 is sensitive to both drugs [2]. Moreover, Ca^{2+} influx through these NSCCs plays a critical role in ET-1-induced mitogenesis [2]. Thus, it is important to elucidate the activation mechanism of NSCCs by ET-1. The biological actions of ET-1 are mediated through ET_ARs and ET_BRs, which belong to a family of G-protein-coupled receptors [3,4]. Therefore, it is important to determine which subtypes of G_α protein are involved in ET-1-induced NSCC activation. To investigate this subject, we confirmed which G_α proteins are coupled with the endothelin receptor in C6 glioma cells. C6 glioma cells predominantly express ET_ARs [2]. ET_ARs are coupled to G_q and G_i, which stimulate PLC and inhibit adenylyl cyclase, respectively [5]. It was reported recently that both

* Corresponding author. Present address: Renal Division, Department of Medicine, Brigham and Women's Hospital and Harvard Medical School, Harvard Institutes of Medicine, Room 520, 77 Avenue Louis Pasteur, Boston, MA 02115, USA. Tel.: +1-617-525-5725; fax: +1-617-525-5830.
E-mail address: ykawanabe@rics.bwh.harvard.edu (Y. Kawanabe).

Abbreviations: $[Ca^{2+}]_i$, intracellular free Ca^{2+} concentration; DMEM, Dulbecco's modified Eagle's medium; ET-1, endothelin-1; ET_ARs, endothelin$_A$ receptors; ET_BRs, endothelin$_B$ receptors; G_{12}G228A/G_{13}G225A, dominant negative mutant of G_{12}/G_{13}; IPs, inositol phosphates; NSCC, nonselective cation channel; PLC, phospholipase C; PTX, pertussis toxin; ROCK, Rho-associated kinase; SOCC, store-operated Ca^{2+} channel.

0006-2952/03/$ – see front matter © 2003 Elsevier Science Inc. All rights reserved.
doi:10.1016/S0006-2952(03)00126-6

ET_ARs and ET_BRs can couple with the G_{12} subfamily, which include G_{12} and G_{13} in NIH3T3 cells [6]. G_{12}/G_{13} has been shown to mediate important signaling pathways such as ROCK-dependent formation of actin stress fibers [7], vascular smooth muscle cell contraction [8], and cell growth [9]. Because G_{12}/G_{13} is also expressed in most cell lines and tissues including the glioma [10–12], and because extracellular Ca^{2+} influx through NSCCs plays an essential role in cell proliferation in C6 glioma cells [2], G_{12}/G_{13} may be involved in the activation of NSCCs. However, it is unclear if ET_ARs couple with G_{12}/G_{13} in C6 glioma cells. To examine this possibility, we used the dominant negative mutant of G_{12}/G_{13} (G_{12}G228A/G_{13}G225A) [8], which inhibits ET-1-induced G_{12}/G_{13}-dependent signaling pathways such as actin stress fiber formation [13]. In this study, we investigated the G_α protein subtypes that may be involved in the ET-1-induced activation of each NSCC in C6 glioma cells. The roles of G_q, G_i, and G_{12}/G_{13} in ET-1-induced Ca^{2+} channel activation were examined using the PLC inhibitor U73122 (1-[6-[((17β)-3-methoxyestra-1,3,5[10]-trien-17-yl)amino]hexyl]-1*H*-pyrrole-2,5-dione), PTX, and G_{12}G228A/G_{13}G225A.

2. Materials and methods

2.1. Cell culture

C6 glioma cells were maintained in DMEM containing 10% fetal bovine serum under a humidified 5% CO_2/95% air atmosphere.

2.2. $[Ca^{2+}]_i$ monitoring

$[Ca^{2+}]_i$ was measured using a fluorescent probe, fluo-3, as described in a previous report [2]. Briefly, C6 glioma cells were loaded with fluo-3 by incubating them with 1 mM fluo-3/acetoxymethyl ester for 30 min at 37° under reduced light. After washing, the cells were suspended at a density of approximately 2×10^7/mL, and 0.5-mL aliquots were used for the measurement of fluorescence by a CAF 110 spectrophotometer (JASCO) with an excitation wavelength of 490 nm and an emission wavelength of 540 nm. At the end of the experiment, Triton X-100 and subsequently EGTA were added at final concentrations of 0.1% and 5 mM, respectively, to obtain the fluorescence maximum (F_{max}) and the fluorescence minimum (F_{min}). $[Ca^{2+}]_i$ was determined from the equilibrium equation $[Ca^{2+}]_i = K_d(F - F_{min})/(F_{max} - F)$, where F was the experimental value of fluorescence and K_d was defined as 0.4 μM [14].

Microfluorimetry of fluo-3 was performed as described previously [15]. Briefly, cells were seeded on 35-mm glass-bottomed plastic dishes (MatTek Corp.), which were marked with a cross to facilitate the localization of injected cells. The cells were loaded with fluo-3 by incubating them with Ca^{2+}-free Krebs-HEPES solution containing 10 μM fluo-3/AM for 30 min at 37° under reduced light. Ca^{2+}-free Krebs-HEPES solution contained: 140 mM NaCl, 3 mM KCl, 1 mM $MgCl_2$, 11 mM glucose, and 10 mM HEPES (pH 7.4, adjusted with NaOH). After washing with the Krebs-HEPES solution (2.2 mM $CaCl_2$ was added to Ca^{2+}-free Krebs-HEPES solution), the cells were kept in fresh Krebs-HEPES solution at 37° for at least 30 min. Fluo-3 microfluorimetry was done at 25° by an Attofluor RatioVision real-time digital fluorescence analyzer (Atto Instruments) equipped with a Carl-Zeiss Axiovert-100 inverted epifluorescent microscope. A 100-W mercury lamp served as the source of excitation. For measurement of $[Ca^{2+}]_i$, fluo-3 was excited at 450–490 nm, and fluorescence was detected at 515–565 nm. $[Ca^{2+}]_i$ was determined as described above.

2.3. Microinjection

Microinjection was performed as described previously [13]. Briefly, cells were seeded onto glass coverslips coated with fibronectin (Iwaki glass), which were marked with a cross to facilitate the localization of injected cells, and incubated overnight in DMEM containing 1% fetal bovine serum. Microinjection of G_{12}G228A/G_{13}G225A, constructed as described previously [13], was performed using a Zeiss microinjection system (Carl Zeiss). All plasmids (100 ng/μL) were used for microinjection into the cell nuclei.

2.4. Drugs

Boehringer Ingelheim K.G. provided LOE 908. Other chemicals were obtained commercially from the following sources: ET-1 from the Peptide Institute; SK&F 96365 from Biomol; and fluo-3/AM from Dojindo Laboratories.

2.5. Statistical analysis

All results are expressed as means ± SEM.

3. Results

3.1. Effects of LOE 908 and SK&F 96365 on the ET-1-induced sustained increase in $[Ca^{2+}]_i$

ET-1 at 10 nM induced a transient and subsequent sustained increase in $[Ca^{2+}]_i$ in C6 glioma cells (Fig. 1). As described previously [2], the sustained phase is due to a transmembrane Ca^{2+} influx, whereas the transient phase is the result of Ca^{2+} mobilization from the intracellular stores. The sustained increase in $[Ca^{2+}]_i$ induced by 10 nM ET-1 was suppressed by SK&F 96365 and LOE 908 in a concentration-dependent manner (Fig. 1). LOE 908 at concentrations ≥ 10 μM completely suppressed this increase (Fig. 1A), whereas the maximal effect of SK&F

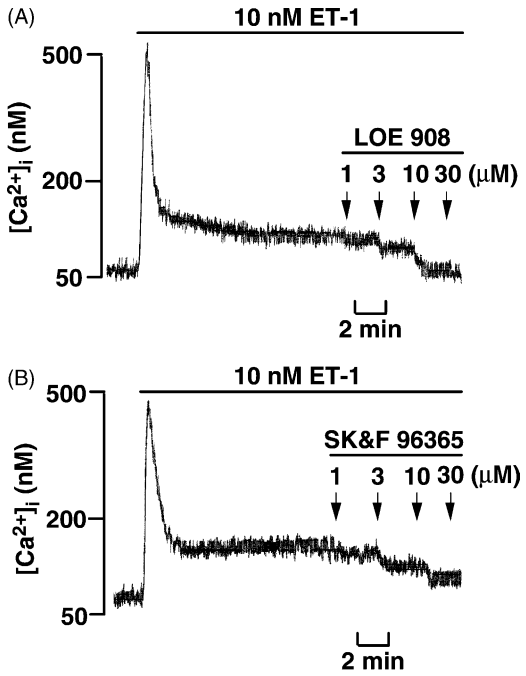

Fig. 1. Original tracings illustrating the effects of various concentrations of LOE 908 (A) or SK&F 96365 (B) on the increase in $[Ca^{2+}]_i$ in C6 glioma cells induced by 10 nM ET-1. The cells loaded with fluo-3 were stimulated by ET-1. After $[Ca^{2+}]_i$ reached a steady-state, increasing concentrations of either LOE 908 or SK&F 96365 were added at the time indicated by the arrows.

96365 was incomplete: about 35% was unsuppressed at concentrations $\geq$ 10 μM (Fig. 1B).

3.2. Effects of PTX on resting and ET-1-stimulated C6 glioma cells

To investigate whether G_i was involved in the activation of Ca^{2+} channels by ET-1, the ET-1-induced sustained increase in $[Ca^{2+}]_i$ was examined in the presence of PTX. PTX (50 ng/mL) failed to inhibit the ET-1-induced sustained increase in $[Ca^{2+}]_i$ (Fig. 2A). In addition, the magnitude of the ET-1-induced sustained increase in $[Ca^{2+}]_i$ in C6 glioma cells pretreated with PTX for 30 min was similar to that observed in control cells upon stimulation of ET-1 in the absence of PTX (data not shown). Moreover, PTX failed to evoke increases in $[Ca^{2+}]_i$ (Fig. 2B).

3.3. Effect of U73122 on ET-1-induced activation of Ca^{2+} channels

ET-1 at 10 nM induced a sustained increase in $[Ca^{2+}]_i$ only in C6 glioma cells treated with 5 μM U73122 (Fig. 3A and B). The transient increase in $[Ca^{2+}]_i$ was not detected in these cells (Fig. 3C). The magnitude of the sustained increase in $[Ca^{2+}]_i$ in U73122-treated cells was around 35% compared to control cells (Fig. 3D). The ET-1-induced sustained increase in $[Ca^{2+}]_i$ was abolished upon treatment with 10 μM LOE 908 (Fig. 3A and D) but not by 10 μM SK&F 96365 (Fig. 3B and D). On the other hand, 5 μM U73343 (1-[6-[((17β)-3-methoxyestra-1,3,5[10]-trien-17-yl)amino]hexyl]-2,5-pyrrolidinedione) failed to inhibit the ET-1-induced increase in $[Ca^{2+}]_i$ (data not shown).

3.4. Effects of G_{12}/G_{13} on ET-1-induced activation of Ca^{2+} channels

We further investigated the effects of G_{12}/G_{13} on Ca^{2+} channels using G_{12}G228A/G_{13}G225A. The ET-1-induced increase in $[Ca^{2+}]_i$ was monitored with microfluorimetry in this experiment. The magnitude of the transient increase in $[Ca^{2+}]_i$ in C6 glioma cells microinjected with G_{12}G228A/G_{13}G225A was similar to that in C6 glioma cells (Fig. 4A). In contrast, ET-1 failed to induce a sustained increase in $[Ca^{2+}]_i$ in C6 glioma cells microinjected with G_{12}G228A/G_{13}G225A (Fig. 4B). On the other hand, the magnitude of the ET-1-induced sustained increase in $[Ca^{2+}]_i$ in C6 glioma cells microinjected with expression plasmids without an insert was similar to that of control cells (data not shown).

4. Discussion

As reported previously [2], the ET-1-induced sustained increase in $[Ca^{2+}]_i$ in C6 glioma cells results from

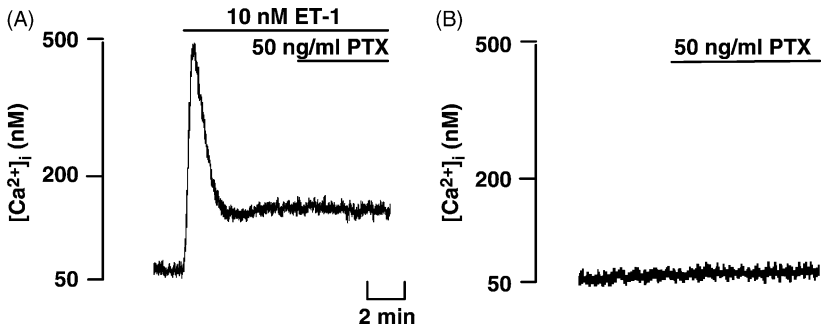

Fig. 2. Original tracings illustrating the effects of PTX on the ET-1-induced sustained increase in $[Ca^{2+}]_i$ in C6 glioma cells (A) and on resting C6 glioma cells (B). The cells were loaded with fluo-3. After $[Ca^{2+}]_i$ reached a steady-state, 50 ng/mL of PTX was added at the time indicated by the horizontal bars.

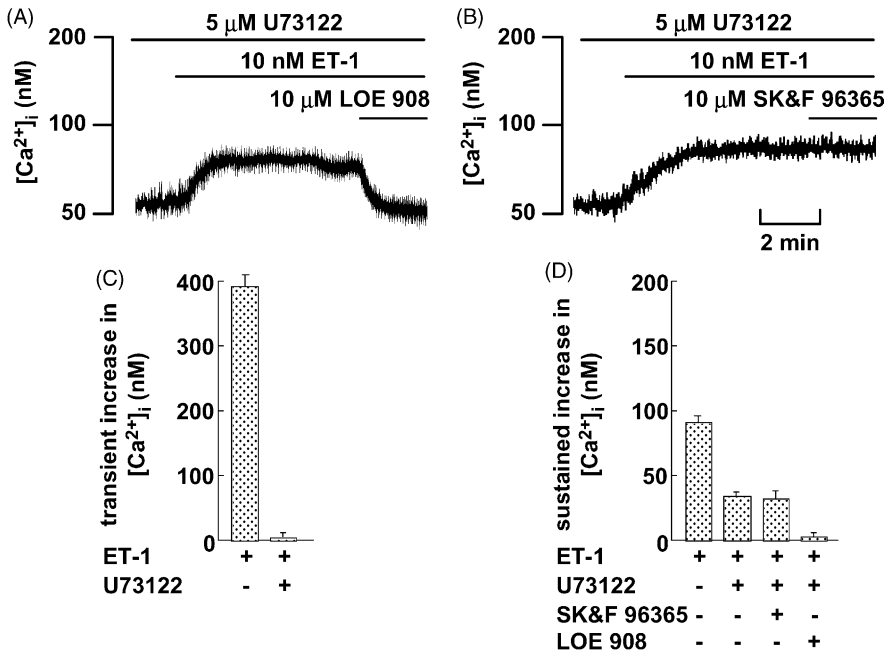

Fig. 3. (A and B) Original tracings illustrating the effects of LOE 908 and SK&F 96365 on the ET-1-induced sustained increase in $[Ca^{2+}]_i$ in C6 glioma cells preincubated with U73122. The cells loaded with fluo-3 were incubated with 5 μM U73122 for 10 min before stimulation with 10 nM ET-1. ET-1 was added at the time indicated by the horizontal bar. After $[Ca^{2+}]_i$ reached a steady-state, 10 μM LOE 908 (A) or 10 μM SK&F 96365 (B) was added. (C and D) Effects of a maximally effective concentration of U73122 (5 μM), LOE 908 (10 μM), or SK&F 96365 (10 μM) on the ET-1-induced transient (C) and sustained (D) increase in $[Ca^{2+}]_i$. The experimental protocols were performed as described in Section 2. Data are presented as means ± SEM of five experiments.

extracellular Ca^{2+} influx through two types of Ca^{2+}-permeable NSCCs (NSCC-1 and NSCC-2). SOCCs do not seem to be activated by ET-1 in C6 glioma cells [2], or in adrenal chromaffin cells [16], unlike vascular smooth muscle cells [15,17]. The ET-1-induced sustained increase in $[Ca^{2+}]_i$ through SOCCs (the LOE 908-resistant and SK&F 96365-sensitive part) was not observed based on the sensitivity to LOE 908 and SK&F 96365 [2]. This difference may be due to a lower formation of IPs and the subsequent incomplete depletion of the intracellular Ca^{2+} store in C6 glioma cells [2]. In resting C6 glioma cells, PTX failed to induce an increase in $[Ca^{2+}]_i$ (Fig. 2B), indicating that PTX has no effects on Ca^{2+} channel activation in these cells. In addition, because PTX failed to affect the ET-1-induced increase in $[Ca^{2+}]_i$ (Fig. 2A), activation of NSCCs by ET-1 does not appear to involve the G_i-dependent pathway. We further examined the role of G_q for activation of NSCCs. It is generally accepted that PLC is activated downstream of G_q [18]. In C6 glioma cells treated with U73122, ET-1 evoked only the sustained increase in $[Ca^{2+}]_i$ (Fig. 3A and B). Therefore, G_q plays an important role in the ET-1-induced transient increase in $[Ca^{2+}]_i$ as described previously [17]. The magnitude of the sustained increase in $[Ca^{2+}]_i$ in U73122-treated C6 glioma cells was around 35% compared with the U73122-untreated C6 glioma cells (Fig. 3D). These results indicate that the ET-1-induced sustained increase in $[Ca^{2+}]_i$ may involve two different pathways, one dependent upon G_q/PLC and the other independent of G_q/PLC. The ET-1-induced sustained increase in $[Ca^{2+}]_i$ was sensitive to LOE 908 and resistant to SK&F 96365 (Fig. 3A and B). Therefore, ET-1 activates only NSCC-1 in C6 glioma cells treated with U73122. These results suggest that activation of NSCC-1 is independent of the G_q/PLC-dependent

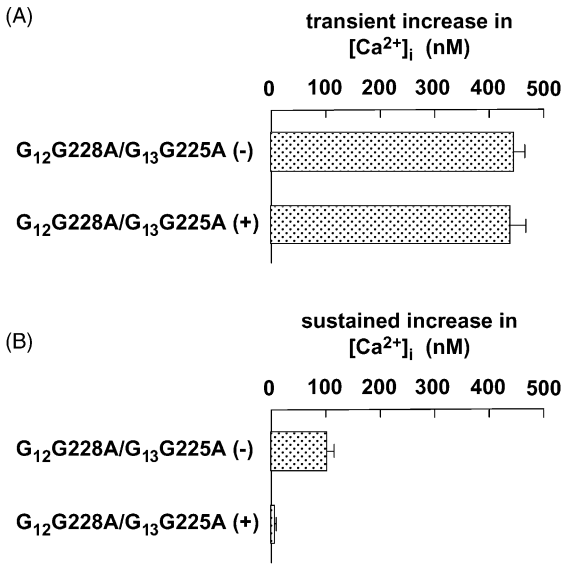

Fig. 4. Effects of $G_{12}G228A/G_{13}G225A$ on the ET-1-induced transient (A) and sustained (B) increase in $[Ca^{2+}]_i$ in C6 glioma cells. Microinjection of $G_{12}G228A/G_{13}G225A$ and fluo-3 microfluorimetry were performed as described in Section 2. Data are presented as means ± SEM of five experiments.

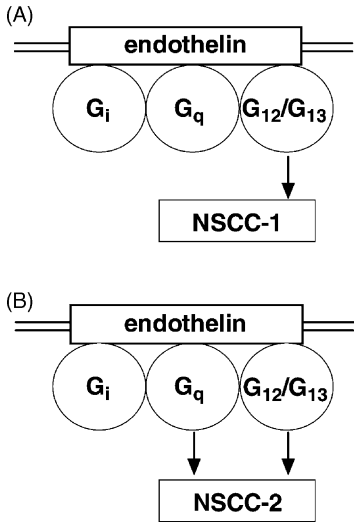

Fig. 5. Schematic representation of signaling pathways for NSCCs activated by ET-1 in C6 glioma cells. ET_ARs couple to G_q, G_i, and $G_{12/13}$ in C6 glioma cells. NSCC-1 is stimulated by ET-1 via the $G_{12/13}$-dependent pathway, whereas NSCC-2 is stimulated by ET-1 via the $G_{12/13}$- and the G_q-dependent pathway. See text for details.

pathway, while activation of NSCC-2 involves a G_q/PLC-dependent pathway (Fig. 5). This suggestion is supported by the following results: ET-1 at 0.1 nM fails to stimulate the formation of IPs, used as an index of inositol trisphosphate formation, and activates only NSCC-1 in C6 glioma cells, while at concentrations $\geq$ 1 nM it stimulates the formation of IPs and activates NSCC-2 in addition to NSCC-1 [2]. Because G_{12}/G_{13} are PTX-insensitive heterotrimeric G proteins, we examined the effects of G_{12}/G_{13} on Ca^{2+} channel activation through the G_q/PLC-independent pathway.

G_{12}G228A/G_{13}G225A inhibits ET-1-induced stress-fiber formation transmitted through the G_{12}/G_{13}-dependent pathway [8,13]. The magnitude of the transient increase in $[Ca^{2+}]_i$ in C6 glioma cells microinjected with G_{12}G228A/G_{13}G225A was similar to that in the intact C6 glioma cells (Fig. 4A). These results indicate that G_{12}/G_{13} are not involved in the ET-1-induced transient increase in $[Ca^{2+}]_i$. In contrast, ET-1 failed to induce a sustained increase in $[Ca^{2+}]_i$ in C6 glioma cells microinjected with G_{12}G228A/G_{13}G225A (Fig. 4B). We conclude that this inhibitory effect is due to G_{12}G228A/G_{13}G225A, because expression plasmids without this insert failed to inhibit the ET-1-induced sustained increase in $[Ca^{2+}]_i$ (data not shown). These results demonstrate that ET_ARs may couple with G_{12}/G_{13} in C6 glioma cells, and the G_{12}/G_{13}-dependent pathway plays an important role in the activation of NSCCs (Fig. 5), while ET-1-induced mobilization of Ca^{2+} from the intracellular Ca^{2+} store may not be involved.

In conclusion, G_q and G_{12}/G_{13} may play important roles for ET-1-induced activation of NSCCs in C6 glioma cells as follows: (a) NSCC-1 activation involves the G_{12}/G_{13}-dependent pathway, and (b) NSCC-2 involves both the G_q/PLC- and the G_{12}/G_{13}-dependent pathway.

Acknowledgments

We thank Boehringer Ingelheim K.G. for donating the LOE 908.

References

[1] Koseki C, Imai M, Hirata Y, Yanagisawa M, Masaki T. Autoradiographic distribution in rat tissues of binding sites for endothelin: a neuropeptide? Am J Physiol 1989;256:R858–66.
[2] Kawanabe Y, Hashimoto N, Masaki T. Ca^{2+} influx through nonselective cation channels plays an essential role in endothelin-1-induced mitogenesis in C6 glioma cells. Neuropharmacology 2001;41:331–40.
[3] Arai H, Hori S, Aramori I, Ohkubo H, Nakanishi S. Cloning and expression of a cDNA encoding an endothelin receptor. Nature 1990; 348:730–2.
[4] Sakurai T, Yanagisawa M, Takuwa Y, Miyazaki H, Kimura S, Goto K, Masaki T. Cloning of cDNA encoding a non-isopeptide-selective subtype of the endothelin receptor. Nature 1990;348:732–5.
[5] Couraud PO, Durieu-Trautmann O, Nguyen DL, Marin P, Glibert F, Strosberg AD. Functional endothelin-1 receptors in rat astrocytoma C6. Eur J Pharmacol 1991;206:191–8.
[6] Mao J, Yuan H, Xie W, Simon MI, Wu D. Specific involvement of G proteins in regulation of serum response factor-mediated gene transcription by different receptors. J Biol Chem 1998;273:27118–23.
[7] Buhl AM, Johnson NL, Dhanasekaran N, Johnson GL. $G\alpha_{12}$ and $G\alpha_{13}$ stimulate RHO-dependent stress fiber formation and focal adhesion assembly. J Biol Chem 1995;270:24631–4.
[8] Gohla A, Offermanns S, Wilkie TM, Schultz G. Differential involvement of $G\alpha_{12}$ and $G\alpha_{13}$ in receptor-mediated stress fiber formation. J Biol Chem 1999;274:17901–7.
[9] Seasholtz TM, Majumdar M, Brown JH. Rho as a mediator of G protein-coupled receptor signaling. Mol Pharmacol 1999;55:949–56.
[10] Strathmann MP, Simon MI. $G\alpha_{12}$ and $G\alpha_{13}$ subunits define a fourth class of G protein α subunits. Proc Natl Acad Sci USA 1991;88:5582–6.
[11] Wilk-Blaszczak MA, Singer WD, Gutowski S, Sternweis PC, Belardetti F. The G protein G_{13} mediates inhibition of voltage-dependent calcium current by bradykinin. Neuron 1994;13:1215–24.
[12] Aragay AM, Collins LR, Post GR, Watson AJ, Feramisco JR, Brown JH, Simon MI. G_{12} requirement for thrombin-stimulated gene expression and DNA synthesis in 1321N1 astrocytoma cells. J Biol Chem 1995;270:20073–7.
[13] Kawanabe Y, Okamoto Y, Nozaki K, Hashimoto N, Miwa S, Masaki T. Molecular mechanism for endothelin-1-induced stress-fiber formation: analysis of G proteins using a mutant $endothelin_A$ receptor. Mol Pharmacol 2002;61:277–84.
[14] Minta A, Kao JPY, Tsien RY. Fluorescent indicators for cytosolic calcium based on rhodamine and fluorescein chromophores. J Biol Chem 1989;264:8171–8.
[15] Zhang XF, Iwamuro Y, Enoki T, Okazawa M, Lee K, Komuro T, Minowa T, Okamoto Y, Hasegawa H, Furutani H, Miwa S, Masaki T. Pharmacological characterization of Ca^{2+} entry channels in endothelin-1-induced contraction of rat aorta using LOE 908 and SK&F 96365. Br J Pharmacol 1999;127:1388–98.
[16] Lee K, Morita H, Iwamuro Y, Zhang XF, Okamoto Y, Miwa S. Failure of endothelin-1 to activate store-operated Ca^{2+} channels by lack of mobilization from intracellular Ca^{2+} stores in cultured bovine adrenal chromaffin cells. Naunyn Schmiedebergs Arch Pharmacol 2001;364: 42–6.
[17] Kawanabe Y, Hashimoto N, Masaki T. Ca^{2+} channels involved in endothelin-induced mitogenic response in carotid artery vascular smooth muscle cells. Am J Physiol Cell Physiol 2002;282:C330–7.
[18] Berridge MJ. Inositol triphosphate and calcium signalling. Nature 1993;361:315–25.